



Cite this: *Nanoscale*, 2026, **18**, 3433

Correction: Layered intercalation ferroelectricity induced by asymmetric ion coordination: a mini-review

Yaxin Gao,^{a,b} Yutong Wang,^{*b} Xuechen Wang^{*b} and Menghao Wu^{*b}

DOI: 10.1039/d6nr90015a

rsc.li/nanoscale

Correction for 'Layered intercalation ferroelectricity induced by asymmetric ion coordination: a mini-review' by Yaxin Gao *et al.*, *Nanoscale*, 2025, **17**, 25477–25483, <https://doi.org/10.1039/D5NR03854E>.

The authors regret the omission of the relevant permission statements for the reproduction of figures from published works in the original article. The updated captions for Fig. 1, 2, 3 and 4 are shown below.

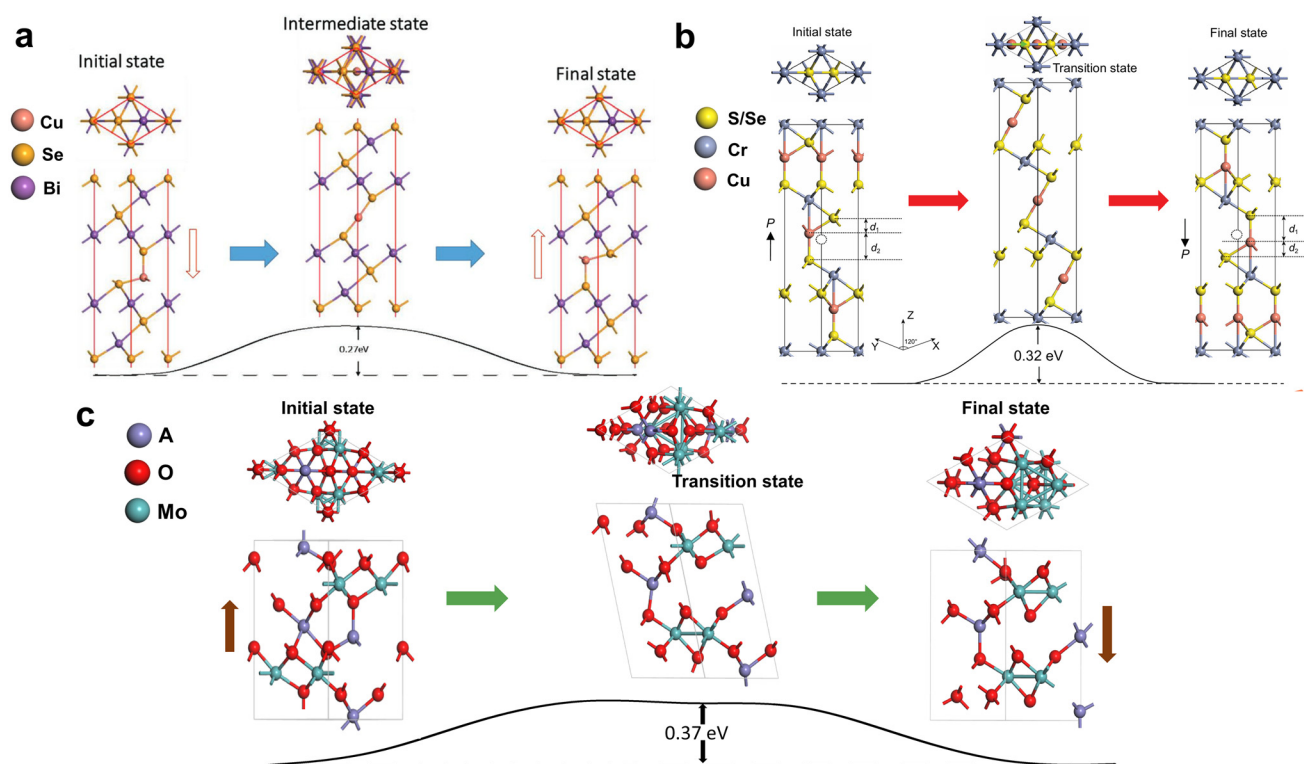


Fig. 1 Ferroelectric switching pathway of (a) 2D $\text{Cu}_x\text{Bi}_2\text{Se}_3$ (reproduced with permission from ref. 18 © WILEY-VCH Verlag GmbH & Co. KGaA, Weinheim, [copyright 2019]), (b) 3D CuCrS_2 (reprinted under a Creative Commons Attribution 4.0 International License¹⁹), and (c) 3D $\text{A}_2\text{Mo}_3\text{O}_8$ (reproduced from ref. 20 with the permission of AIP Publishing) via the combination of in-plane and out-of-plane displacements of intercalated metal ions, where the polarizations stem from the tetra-coordination of Cu or A ions.

^aSchool of Physics and Mechanical Electrical & Engineering, Institute of Astronomy and High Energy Physics, Hubei University of Education, Wuhan, Hubei 430205, China

^bSchool of Physics, Huazhong University of Science and Technology, Wuhan, Hubei 430074, China. E-mail: 1393375834@qq.com, 814095206@qq.com, wmh1987@hust.edu.cn



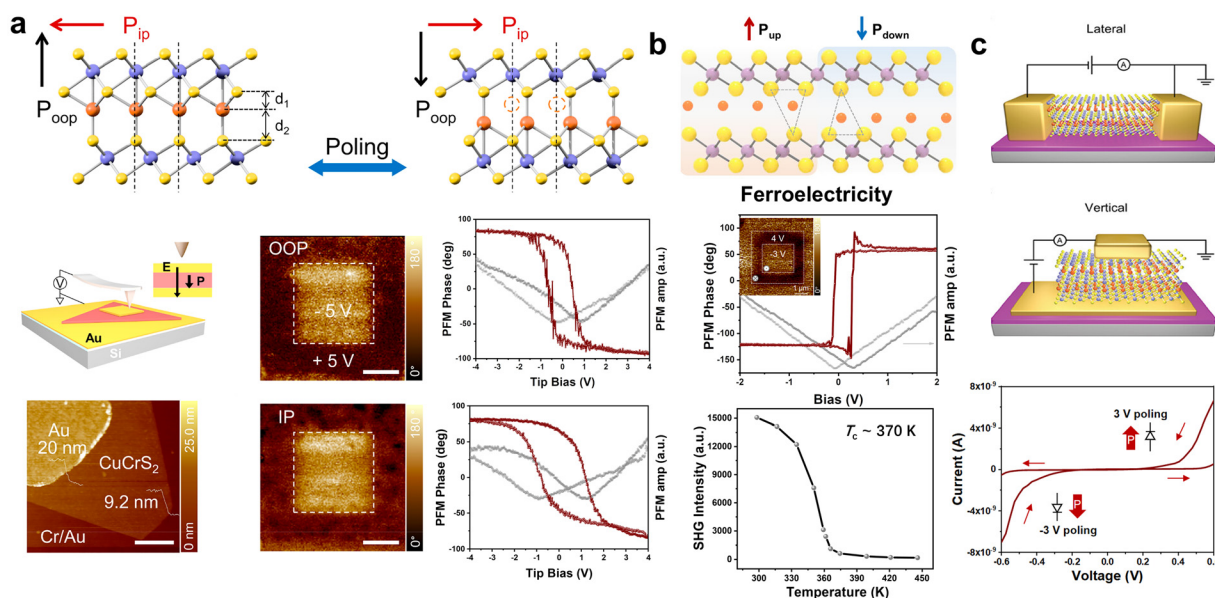


Fig. 2 (a) Illustration and height profiles of the Au-encapsulated CuCr_2S_2 flake on a SiO_2/Si substrate covered with a conductive layer of Cr/Au , and OOP and IP phase images after forward (-5 V) and reverse ($+5\text{ V}$) DC bias, and the corresponding ferroelectric hysteresis loops. Reproduced with permission from ref. 9 © [2022] American Chemical Society. (b) PFM phase and amplitude hysteresis loop of the CuScS_2 nanosheet and temperature-dependent optical SHG measurement. Reprinted under a Creative Commons Attribution 4.0 International License.¹¹ (c) Schematic diagram of lateral and vertical devices based on the AgCrS_2 nanosheet, and I - V curves of the lateral AgCrS_2 ferroelectric diode device after applying opposite poling voltages (3 V and -3 V). Reproduced with permission from ref. 21 © WILEY-VCH Verlag GmbH & Co. KGaA, Weinheim, [copyright 2024].

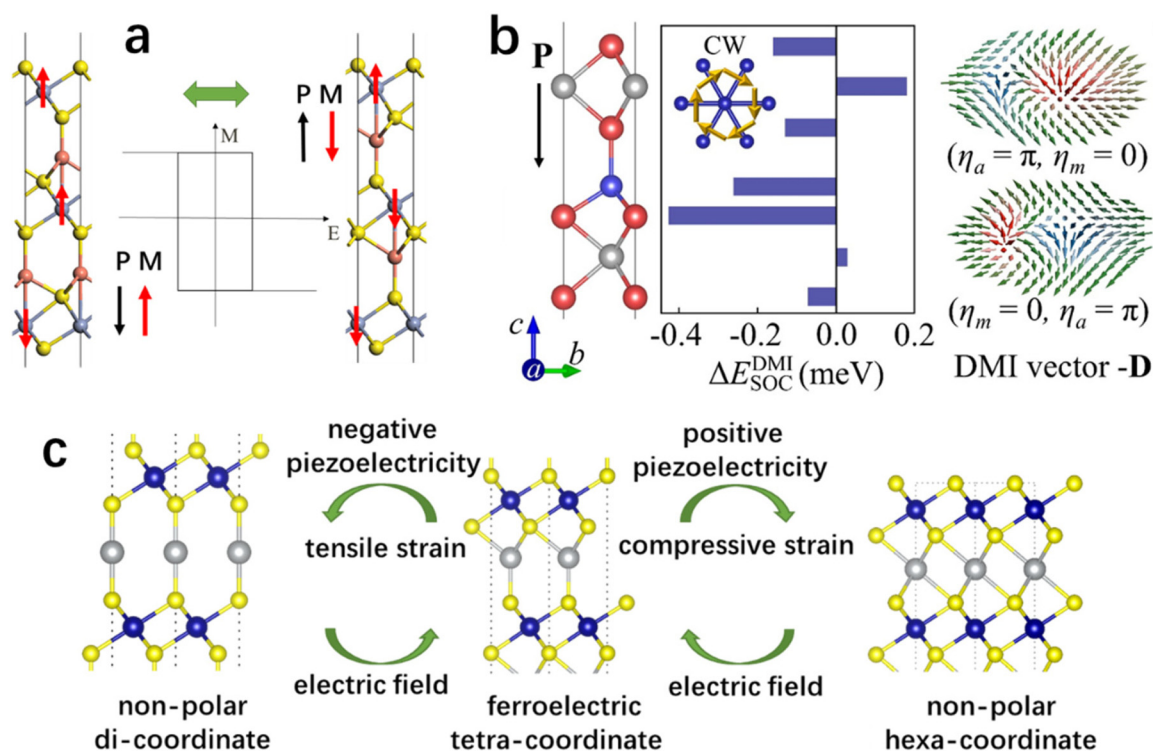


Fig. 3 (a) The change of spin distribution upon FE switching for trilayer CuCr_2S_2 , where black and red arrows in the sketches of M - E loops denote the direction of polarization and magnetization, respectively. Reprinted under a Creative Commons Attribution 4.0 International License.¹⁹ (b) $\text{Co}(\text{MoTe}_2)_2$ monolayer with atomically resolved spin-orbit-coupling (SOC) energy associated with DMI, and two bimerons with opposite helicities corresponding to the same DMI vector $-\mathbf{D}$. Reproduced from ref. 27 with the permission of APS Publishing. (c) Illustration of phase transitions for AgCrX_2 driven by strain or an electric field, respectively giving rise to piezoelectricity and electrostrain. Reproduced with permission from ref. 28 © [2024] American Chemical Society.



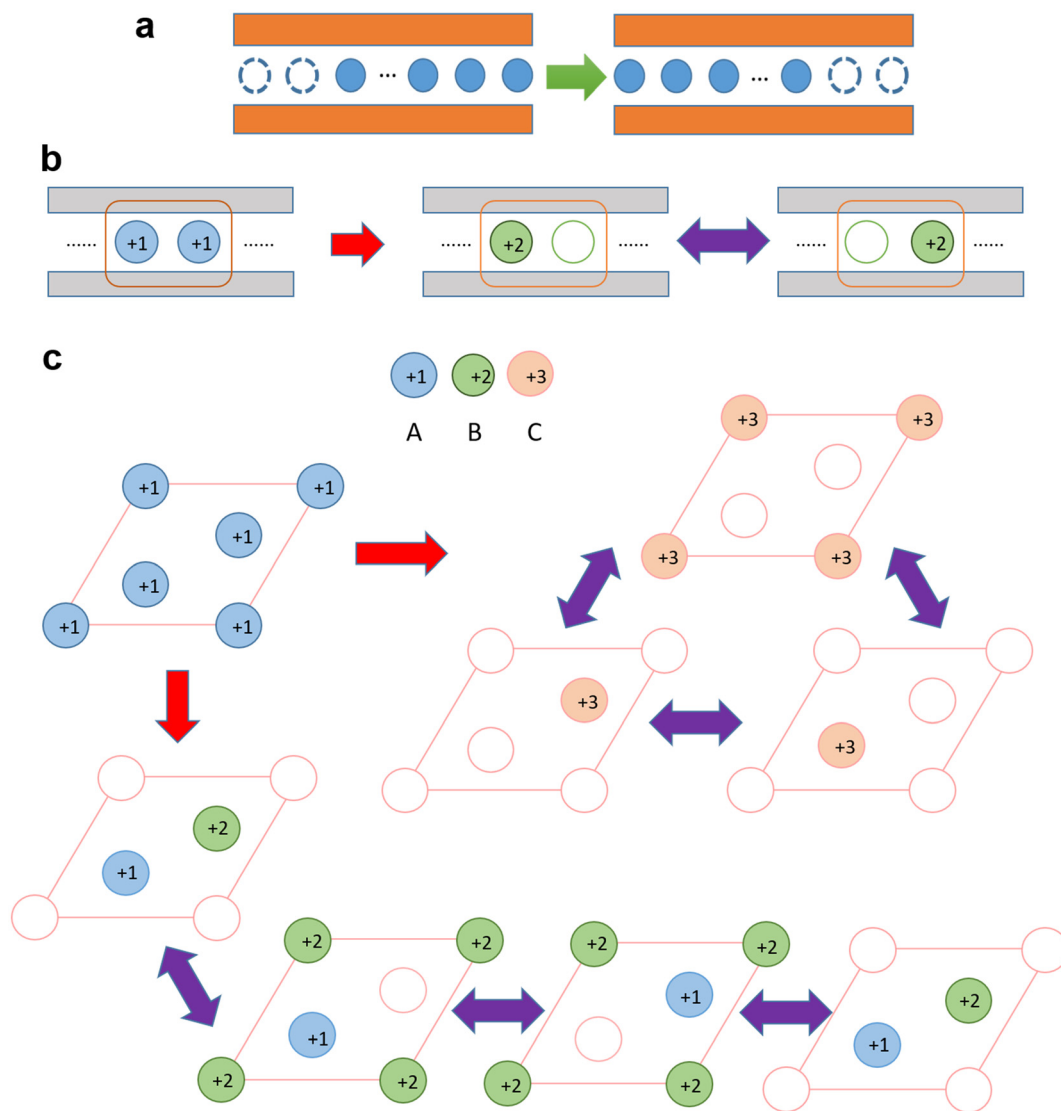


Fig. 4 (a) Schematic diagram of migration for the intercalated ions (denoted by blue spheres) along the conducting channel with ion vacancies, which gives rise to quantized ferroelectricity. Reproduced with permission from ref. 36 © [2022] American Chemical Society. (b) The conversion from layered AMX_2 to $B_{0.5}MX_2$ by the cation-exchange reaction and its ferroelectric switching pathway between bi-stable polar states (side view of the unit cell), where the displacement of B ions is equivalent to \mathcal{M} mirror reflection operation to the lattice. (c) Similar conversion from AMX_2 to $C_{1/3}MX_2$, $A_{1/3}B_{1/3}MX_2$ and their ferroelectric switching pathways between various equivalent polar states (top view of the unit cell), where ion displacements are equivalent to C_3 rotation operation. Reproduced from ref. 37 with permission from the Royal Society of Chemistry.

The Royal Society of Chemistry apologises for these errors and any consequent inconvenience to authors and readers.

